It Doesn't Look Like Anything to Me:
Using Diffusion Model to Subvert Visual Phishing Detectors

Supplementary Materials

Qingying Hao
UIUC
qhao2@illinois.edu

Nirav Diwan
UIUC
ndiwan2@illinois.edu

Ying Yuan
University of Padua
ying.yuan@math.unipd.it

Giovanni Apruzzese
University of Liechtenstein
giovanni.apruzzese@uni.li

Mauro Conti
University of Padua
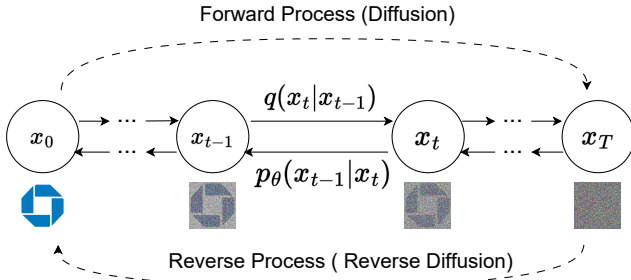mauro.conti@unipd.it

Gang Wang
UIUC
gangw@illinois.edu

Figure 1: **Diffusion Model**—The forward process (q) adds Gaussian noises to the image at each step. The reverse process learns a denoise function p_θ to re-generate the clean image from noise.

1 Diffusion Models

Basic Diffusion Model. Denoising diffusion probabilistic models (DDPM) (referred to as "diffusion models" for short) are generative models that generate high-quality images while offering fine-grained controls over image fidelity and diversity [6, 10, 11]. The goal of a diffusion model is to learn to generate data similar to the training data. To do so, diffusion models "destroy" the training data by progressively adding Gaussian noise to the image, and then learn to recover the original image by reversing the noising process. As shown in Figure 1, it contains a forward (diffusion) process and a reverse (diffusion) process. The forward process is to add Gaussian noise to a clean image step by step until reaching a version of (close to) pure Gaussian noise. The reverse diffusion process is defined by a Markov chain to transform Gaussian noise back to a clean image. The goal is to learn the reverse process with a neural network p_θ.

More specifically, during the forward process, we take x_0 (i.e., a clean image) and apply q to add Gaussian noises at each timestamp t to produce a series of latent vectors from x_1 to x_T, with variance $\beta_t \in (0,1)$. This process is modeled by a Markov chain to obtain the approximate posterior:

$$q(x_1,...,x_T|x_0) := \prod_{i=1}^{T} q(x_t|x_{t-1}) \qquad \text{(Eqn. 1)}$$

$$q(x_t|x_{t-1}) := N(x_t; \sqrt{1-\beta_t}x_{t-1}, \beta_t \mathbf{I}) \qquad \text{(Eqn. 2)}$$

Given a large T and well-scheduled variance βt, x_T is nearly an isotropic Gaussian distribution N [11]. A recent work [6] shows that we do not need to repeatedly sample from $x_t \sim q(x_t|x_0)$. Instead, with $\alpha_t := 1$-β_t and $\bar{\alpha}_t := \prod_{s=0}^{t} \alpha_s$, we can calculate x_t as:

$$x_t = \sqrt{\bar{\alpha}_t}x_0 + \sqrt{1-\bar{\alpha}_t}\varepsilon, \varepsilon \sim N(0, \mathbf{I}) \qquad \text{(Eqn. 3)}$$

Here, $1-\bar{\alpha}_t$ defines the variance of the noise ε at an arbitrary timestamp t. Using Bayes theorem, the posterior $q(x_{t-1}|x_t, x_0)$ can also be presented as a Gaussian and calculated with mean $\mu_q(x_t, x_0)$ and variance $\beta_{q(t)}$ [11] which:

$$\tilde{\mu}(x_t, x_0) := \frac{\sqrt{\bar{\alpha}-1}\beta_t}{1-\bar{\alpha}_t}x_0 + \frac{\sqrt{\alpha_t}(1-\bar{\alpha}_{t-1})}{1-\bar{\alpha}_t}x_t \qquad \text{(Eqn. 4)}$$

$$\tilde{\beta}_t := \frac{1-\bar{\alpha}_{t-1}}{1-\bar{\alpha}_t}\beta_t \qquad \text{(Eqn. 5)}$$

$$q(x_{t-1}|x_t, x_0) = N(x_{t-1}; \tilde{\mu}(x_t, x_0), \tilde{\beta}_t \mathbf{I}) \qquad \text{(Eqn. 6)}$$

For the inverse process, to recover $q(x_0)$, we can sample from $q(x_T) \sim$ Gaussian $N(0, \mathbf{I})$ and run the reverse distribution $q(x_t|x_{t-1})$ until we reach x_0. The reverse process could be approximated using a neural network to predict a mean μ_θ and variance Σ_θ as follows:

$$p_\theta(x_{t-1}|x_t) := N(x_{t-1}; \mu_\theta(x_t, t), \Sigma_\theta(x_t, t)) \qquad \text{(Eqn. 7)}$$

In DDPM [6], the variance is fixed at each time t as a function of the α coefficient defined by Eqn. 5. The variance can also be predicted as Σ_θ using the neural network [11]. To train the model p_θ, we can optimize the variational lower-bound L_{vlb} to get $p_\theta(x_0)$ as follows:

$$L_{vlb} = L_0 + L_1 + ... + L_{T-1} + L_T \qquad \text{(Eqn. 8)}$$

$$L_0 = -\mathbb{E}_{q(x_1|x_0)}[\log p_\theta(x_0|x_1)] \qquad \text{(Eqn. 9)}$$

$$L_T = D_{KL}(q(x_T|x_0)||p(x_T)) \qquad \text{(Eqn. 10)}$$

$$L_{t-1} = \sum_{t=2}^{T} \mathbb{E}_{q(x_t|x_0)}[D_{KL}(q(x_{t-1}|x_t,x_0)||p_\theta(x_{t-1}|x_t)))] \qquad \text{(Eqn. 11)}$$

Note that, only L_{t-1} has trainable parameters—It is simpler for training the diffusion model by focusing on this L_{t-1} term [6]. This is referred to as simplified objective function $L_{simple}(\theta)$. So the goal of training is to minimize the difference between the learned denoising transition step $p_\theta(x_{t-1}|x_t)$ and the forward process posteriors $q(x_{t-1}|x_t,x_0)$ as the ground truth defined by their KL Divergence.

According to the KL Divergence between two Gaussian distributions, the optimization of L_{simple} is presented by Eqn. 12.

$$\arg\min_\theta D_{KL}(q(x_{t-1}|x_t,x_0)||p_\theta(x_{t-1}|x_t)),$$
$$= \arg\min_\theta D_{KL}(N(x_{t-1};\tilde{\mu},\Sigma_q(t)||N(x_{t-1};\mu_\theta,\Sigma_q(t)))$$
$$= \arg\min_\theta \frac{1}{2\sigma_q^2(t)}[||\mu_\theta - \tilde{\mu}||^2] \qquad \text{(Eqn. 12)}$$

In the basic DDPM [6], the variance for forward and reverse processes are fixed at each time t and can be calculated as a function of α coefficient. We can write both of the variances $\beta_t\mathbf{I}$ and $\tilde{\beta}_t\mathbf{I}$ as $\Sigma_q(t)$ for brevity [10]. The variance could be written as $\Sigma = \sigma_q^2(t)\mathbf{I}$, using Eqn. 5.

One way to optimize the loss function is to train a neural network to predict $\mu_\theta(x_t,t)$. Alternatively, the network can predict x_0 and use Eqn. 4 to get $\mu_\theta(x_t,t)$. In practice, training the network to predict the noise ε gives better image quality [6]. So the simplified objective is defined as:

$$L_{simple} = \mathbb{E}_{t,x_0,\varepsilon}[||\varepsilon - \varepsilon_\theta(x_t,t)||^2] \qquad \text{(Eqn. 13)}$$

$\mu_\theta(x_t,t)$ can be derived from $\varepsilon_\theta(x_t,t)$ as:

$$\mu_\theta(x_t,t) = \frac{1}{\sqrt{\alpha_t}}(x_t - \frac{1-\alpha_t}{1-\sqrt{\bar{\alpha}_t}}\varepsilon_\theta(x_t,t)) \qquad \text{(Eqn. 14)}$$

Improved Diffusion Model. The improved diffusion model [11] reduces the sampling by an order of magnitude during the forward passes without sacrificing the quality of generated images. Instead of fixing $\Sigma_\theta(x_t,t) = \sigma_t^2\mathbf{I}$, the improved diffusion model also learns the variance for the reverse process to improve the log-likelihood (for $\log p(x)$). It defines the learning of variances as follows:

$$\Sigma_\theta(x_t,t) = \exp(v\log\beta_t + (1-v)\log\tilde{\beta}_t) \qquad \text{(Eqn. 15)}$$

where β_t and $\tilde{\beta}_t$ represent the upper and lower bounds for the reverse process variances, and v is the predicted variance from the neural network. The improved diffusion model proposes a new hybrid loss which predicts for both mean $\mu_\theta(x_t,t)$ and variance $\Sigma_\theta(x_t,t)$:

$$L_{hybrid} = L_{simple} + \lambda L_{vlb} \qquad \text{(Eqn. 16)}$$

Brand	# Bypass (# tested)	Rate
Amazon	40 (40)	1.00
AT&T	18 (18)	1.00
BOA	40 (40)	1.00
Chase	40 (40)	1.00
CIBC	26 (26)	1.00
DHL	41 (41)	1.00
DocuSign	36 (36)	1.00
Dropbox	40 (40)	1.00
eBay	37 (37)	1.00
Google	25 (25)	1.00
Netflix	16 (16)	1.00
Outlook	40 (40)	1.00
PayPal	40 (40)	1.00
Spotify	40 (40)	1.00
Yahoo	8 (8)	1.00
LinkedIn	39 (40)	0.98
Comcast	27 (29)	0.93

Table 1: **Gradient-Masking Defense**—Number and rate of adversarial pages that bypass PhishIntention after gradient masking.

λ is the scaling factor (set to be small so the L_{vlb} will not overwhelm L_{simple}). It also applies a stop gradient to $\mu_\theta(x_t,t)$ for the L_{vlb} term such that L_{vlb} only influences $\Sigma_\theta(x_t,t)$.

2 Gradient-Masking

Another defense method proposed by prior work [8, 9] is gradient masking. The goal is to modify the phishing detection model such that it becomes more difficult for optimization-based algorithms to generate adversarial examples. More specifically, by changing the activation function of the phishing detector to a "smooth" version (similar to defensive distillation [3]), we expect to increase the difficulty of searching the gradients for computing adversarial examples. We test the gradient-masking method used in [8], using a *Step ReLu* function: $f(x) = max(0, \alpha \cdot \lceil \frac{x}{\alpha} \rceil)$. We replace all the ReLu functions in the OCR-Siamese model with the Step ReLu function. We then test this improved version of PhishIntention end-to-end on webpage levels using the same 20% of testing data. The results are shown in Table 1.

We find that gradient-masking is not effective in defending against LogoMorph. Most of our adversarial webpages can still bypass PhishIntention. The reason is that our adversarial logos "attack" the similarity function to compare the input and reference logos. It relies on font manipulation and a diffusion model to introduce *large* and yet semantic-preserving perturbations. Gradient masking, on the other hand, is designed to defend against classification-gradient-based adversarial examples (that introduce small noises), which is not well suited to defend against our attack. Noteworthy is that also Phish-GAP [7] defeated detectors using *Step ReLu*.

3 Additional Visual Examples

Figure 2 shows examples of successful adversarial logos produced by PhishGap. Figures 3–4 show example adversarial
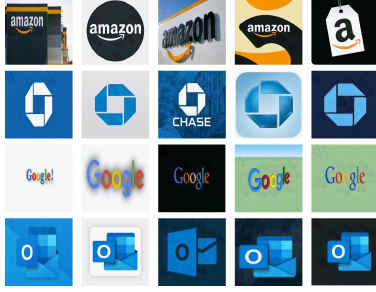
(a) Example 1
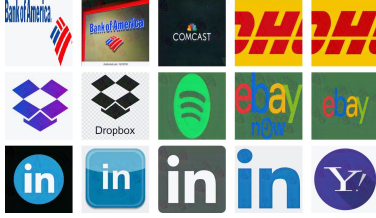
(b) Example 2

Figure 2: **Examples of Successful PhishGap Attacks**—While these logo images succeed in bypassing PhishIntention, they are not necessarily ready to be added to webpages to deceive users end-to-end due to image cropping, disproportionate stretching, unusual background color, and the use of non-web logos.

logos produced by our system. Figures 5–7 show example webpages with our adversarial logos that bypassed the target PhishIntention detector.

4 SpacePhish Experiment

We follow an existing method (SpacePhish [1]) to generate adversarial phishing webpages that were originally designed to bypass HTML-based detectors. Then we test these adversarial phishing pages against a logo-based visual phishing detector, PhishIntention [9]. The goal is to understand if PhishIntention can detect such adversarial phishing webpages.

First, we follow the same method described in [1] to generate adversarial webpages. This process starts by first training a target phishing detector with a Random Forests (RF) classifier using HTML features. The classifier is trained with a dataset of 30K websites (15K benign and 15K phishing) [4]. The classifier uses 80% of the data for training and the rest 20% for testing. After training, the classifer is very accurate, with a true positive rate (TPR) of 0.98 and a false positive rate (FPR) of 0.04. Then, we randomly selected 1k phishing websites from the testing set for adversarial manipulation. Utilizing the methods proposed in [1] (i.e., adding links or wrapping all links with "onclick"), we generate 160 adversarial webpages. These adversarial webpages can bypass the RF classifier with 100% evasion success rate.

(a) Image-Only Logo

Figure 3: **Examples of Successful Attacks**— We show successful examples of (a) image-only logos. These logos have a similarity range of $0.6 - 0.87$. From left to right, the quality decreases.

Then, we run PhishIntention [9] on these 160 adversarial phishing webpages, which are mimicking 34 brands in PhishIntention's reference list (i.e., protected brands). Only 27% of these samples managed to bypass the detection of PhishIntention. The result indicates that PhishIntention has good resistance against such adversarial phishing pages that focus on manipulating HTML (provided that the corresponding webpages are included in the reference list!).

5 Additional Analysis of Main User Study

We perform an additional analysis of the data collected from our main user study. Table 2 shows the demographics and background information of participants. We want to examine whether users's phishing knowledge, technical background in Computer Science and Engineering (CSE), and their brand familiarity would affect their detection performance on *adversarial phishing pages*. We did not perform the analysis for "technical background in computer security" because the vast majority of users (95%) do not have such background.

Does Expertise with IT Affect `LogoMorph`**?** We report the overall accuracy, true positive rate (TPR), and true negative rate (TNR) for users in different groups in the *adversarial*

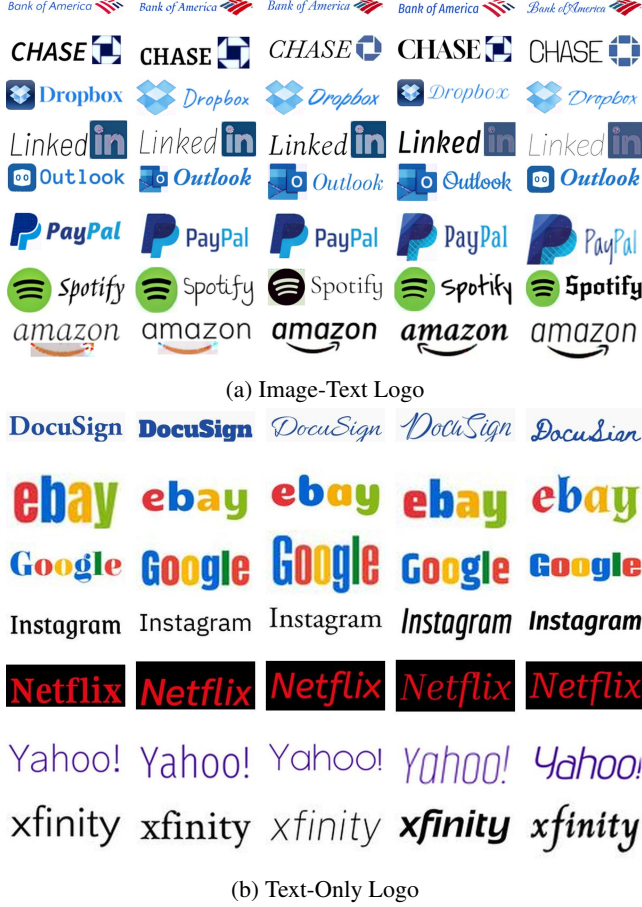(a) Image-Text Logo

(b) Text-Only Logo

Figure 4: **Examples of Successful Attacks**— We show successful examples of (a) image-text logos and (b) text-only logos. These logos have a similarity range of $0.6 - 0.87$. From left to right, the quality decreases.

User Study	Adv. Attack	Baseline	Total
Gender			
Male	52	24	**76**
Female	47	23	**70**
Non-binary / third gender	1	3	**4**
Age			
18-29	23	15	**38**
30-39	32	14	**46**
40-49	18	5	**23**
50-59	15	9	**24**
60-69	8	5	**13**
70 or above	4	2	**6**
Education			
Some high school or less	0	1	**1**
High school diploma or GED	11	1	**12**
Some college, but no degree	22	11	**33**
Associates or technical degree	15	8	**23**
Bachelor's degree	35	22	**57**
Graduate or professional degree	17	7	**24**
Phish knowledge			
Yes	68	36	**104**
No	29	13	**42**
Prefer not to say	3	1	**4**
Technical Background in Computer Science / Engineering			
Yes	14	10	**24**
No	84	39	**123**
Prefer not to say	2	1	**3**
Technical Background in Computer Security			
Yes	3	2	**5**
No	96	46	**142**
Prefer not to say	1	2	**3**
Total	100	50	**150**

Table 2: **Demographics of our main user studies.**

study in Table 3. Users are divided into different groups based on whether they have phishing knowledge and a technical background in CSE. We find that the technical background in CSE does not affect users' detection rate of adversarial phishing pages (TPR=0.59 for users with CSE background, and TPR=0.60 for users without CSE background). Although the TNR of users without CSE background (TNR=0.79) is slightly higher than that of users with CSE background (TNR=0.73), this difference is not statistically significant (p=0.1, χ^2=2.70). The same conclusion holds for users with phishing knowledge: whether or not users have phishing knowledge does not statistically affect their performance on adversarial phishing pages (TPR). However, the result of our Chi-squared statistic test indicates that people with phishing knowledge are more likely to correctly identify benign webpages (p=0.02, χ^2=5.29).

**Impact of Brand Familiarity.** We also analyze the correlation between users' detection performance and their brand familiarity. In our adversarial study in the main paper, we captured 1,800 responses, and 85.7% (1,542) indicated that users know the brands. Users knowing the brand get TPR=0.60 and TNR=0.81; in contrast, users who do not know the brand get TPR=0.54 and TNR=0.66. Based on the Chi-squared statistic test, no evidence suggests that brand familiarity would significantly affect users' performance on detecting adversarial phishing webpages (p=0.20, χ^2=1.66). However, users who know the brand are more likely to correctly identify legitimate webpages (p<0.001, χ^2=13.12).

Discussion. The result indicates that the effectiveness of `LogoMorph` is not affected by users' technical background in CSE, phishing knowledge, or brand familiarity. However, phishing knowledge and brand familiarity can help users recognize legitimate web pages. This finding is interesting in light of a recent work [5], wherein a user study (n=126) was carried out to assess the ability of individuals to recognize "adversarial webpages from the wild web" (i.e., without using `LogoMorph`). In this study, users with expertise in IT performed better than "amateurs". It can hence be said that `LogoMorph` is a subtle threat, since it can fool users independently from their background. In contrast, other forms of
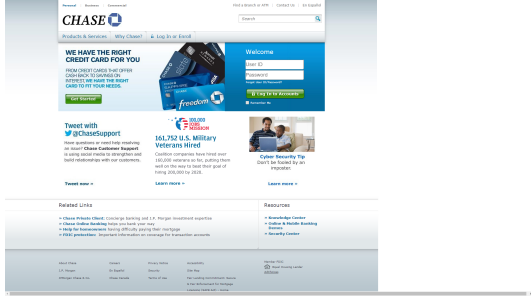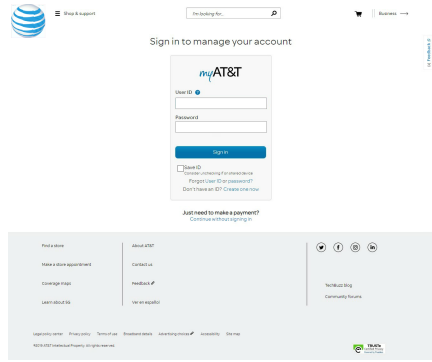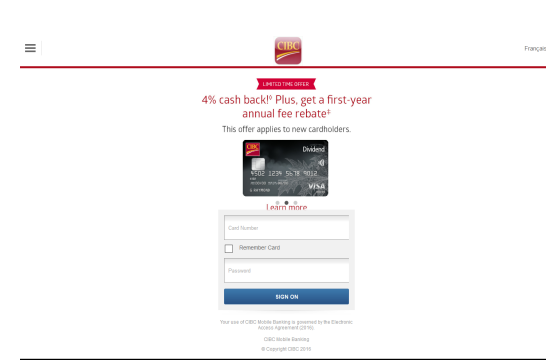
(a) Chase Bank
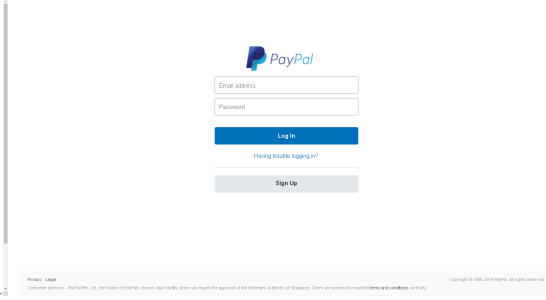
(b) PayPal

Figure 5: **Phishing Page with Image-Text Logo Attack**—Successful phishing pages that bypass PhishIntention, with the combined adversarial image-text logos inserted into the target webpages of CHASE Bank and PayPal.
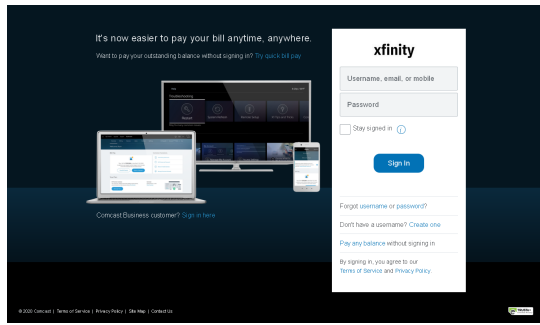

(a) AT&T

(b) CIBC Bank

Figure 6: **Phishing Page with Image Logo Attack**—Successful phishing pages that bypass PhishIntention, with adversarial image logos inserted into the target webpages of AT&T and CIBC Bank.

Figure 7: **Phishing Page with Text Logo Attack**—Successful phishing pages that bypass PhishIntention, with attack fonts inserted into the target screenshots of Comcast page.

adversarial webpages, such as those employed by real phishers [5], can be more easily spotted by IT experts.[1]

---

[1]Abundant prior work has carried out user studies on phishing (for a recent survey, see [2]), but the work by Draganovic et al. [5] is the only one that considers adversarial webpages and collects information on the IT expertise of their participants (the latter was not provided in PhishGAP [7]).

Users technical background	Accuracy	TPR	TNR
With tech background of CSE	0.66	0.59	0.73
Without tech background of CSE	0.70	0.60	0.79
With phish knowledge	0.70	0.59	0.81
Without phish knowledge	0.67	0.60	0.74

Table 3: **Results of Users with Different Technical Background**—We report the accuracy, TPR and TNR for people with/without phishing knowledge and technical background in Computer Science and Engineering in the *adversarial study*.

6 Ancillary User Study (Logo-Level)

We report additional analysis from our ancillary user study at the logo level.

Per-Brand Analysis. We find it instructive to analyze the human-rated resemblance on a brand-by-brand basis. To this purpose, we show in Figure 8 the human-rated resemblance of the *best* category of logos for each brand. We can see that, in general, the human-rated resemblance is highest for the logos having $0.8 \leq \text{Sim} < 0.87$. However, for three brands
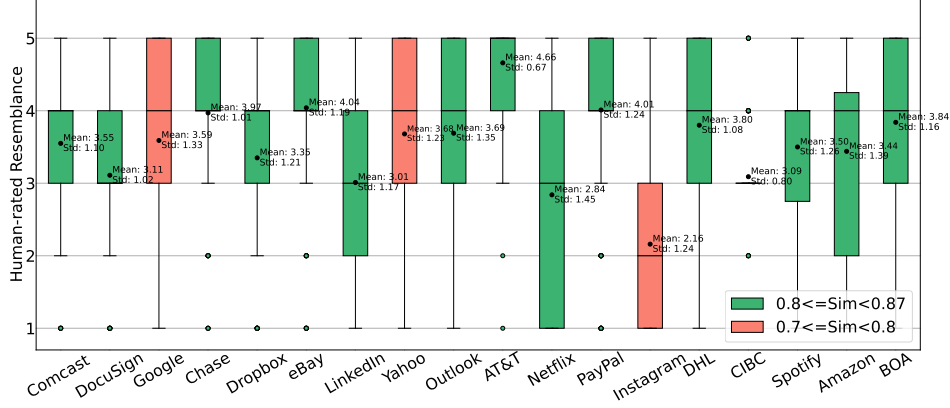
Figure 8: **Per-brand Results of our Logo-level User Study**—We show, for each targeted brand, the "best category" of adversarial logos, i.e., those with the highest human-rated resemblance. For three brands (Google, Yahoo, Instagram), our participants deem that logos with a lower similarity (according to PhishIntention) have a better resemblance with the targeted brands.
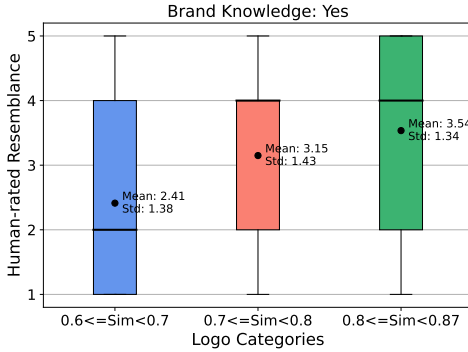

Figure 9: **Main Results of our Logo-level User Study**—Distribution of the human-rated resemblance (higher is better) across adversarial logos crafted with `LogoMorph`. Each bin corresponds to logos that achieve a given similarity (according to PhishIntention) with the "original" logo of the targeted brand. We only report the answers of participants who are familiar with the targeted brand.
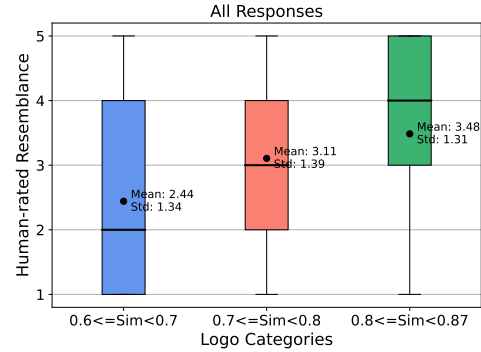

Figure 10: **All Responses of Our Logo-Level User Study**—We consider the responses of those users who know the targeted brands, and those who do not (combining Figures 9 and 11).

(Google, Yahoo, Instagram), our participants rated logos having $0.7 \leq \mathrm{Sim} < 0.8$ with a higher resemblance than those having $0.8 \leq \mathrm{Sim} < 0.87$. We find this result intriguing, suggesting that *the similarity metric used by PhishIntention (to compare any logo with a "benign" logo of a given brand) may not fully align with the way human users perceive whether a logo resembles its intended brand*. This result may also be inspiring for future research, since it may drive the development of novel metrics to compute the similarity. Nevertheless, another interesting result shown in Figure 8 is that, even though the overall human-rated resemblance (for $0.8 \leq \mathrm{Sim} < 0.87$) has an average of 3.54, the adversarial logos of some brands exhibit a remarkably high resemblance. For instance, the average human-rated resemblance for AT&T is 4.86, whereas the one for eBay and PayPal is above 4.

Knowledge of the Brand. We also report the results of our user study by considering our full responses (i.e., without removing the responses of users who do not know the brand),

shown in Figure 10; and those of users who do not know the targeted brand, shown in Figure 11. For Figure 11, the green and orange boxplots each include 171 responses and the blue one has 170. For Figure 10 the green and orange boxplots each have 1,800 responses and the blue one has 1,600. Given that only few users did not know our brands (which we chose among those being most popular in the U.S.—*thereby proving that our choice of brands to consider in our main paper is well-founded*), there is a negligible difference between people who know the brand (Figure 9) and the overall result (Figure 10). Finally, by turning the attention at Figure 11, we see that these users were mostly unsure (which makes sense since they did not know the brand).

Comparison with PhishGAP [7]. We stress that all these results only capture how well a given user rates the *logo in isolation*—and cannot be used to determine if users are "fooled" by such logos (since the logos must be put in web-pages). This is why, in our main paper, we have carried out another user study showing entire webpages to our partici-pants. We note that PhishGAP [7] also carried out user studies at the logo level. Specifically, the authors of [7] assessed how
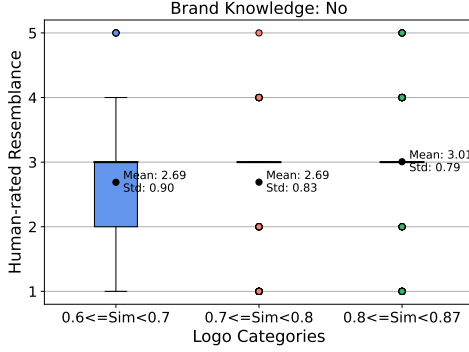
Figure 11: **Responses from of Users Who Do Not Know the Brands**—Less than 10% of our responses are made by users who do not know the brand represented by the (adversarial) logo.

well their proposed adversarial logos could fool humans via a questionnaire containing various pairs of logos: an "adversarial logo" (crafted via PhishGAP [7]) and an "original" logo. Participants (i.e., 30 university students, and 287 MTurk workers) were asked to rate how similar the two logos were: ideally, the more similar they were, the more likely that the "adversarial logo" could have fooled a human user. The results showed that, on average, users rated the pairs above the middle-point, demonstrating that PhishGAP's logos can deceive humans. However, the major limitation of this study is that it only focuses on the logo level: as we showed in the main paper, only 5.5% of the logos generated by PhishGAP can bypass PhishIntention end-to-end. Hence, despite showing that the logos of PhishGAP can deceive humans, human users would not see these logos in the first place since the majority would be blocked by Phishintention. In contrast, our main user study is done by selecting adversarial webpages that bypassed Phishintention end-to-end, thereby allowing to gauge the real threat of `LogoMorph` to human users.

> **Takeaway.** From this user study, we have learned three lessons. First, as long as the adversarial logos can bypass the detector, choosing logos with a higher similarity is the most sensible way to use `LogoMorph`. Second, the similarity metric used by PhishIntention may not always align with the way human users perceive whether a logo resembles its brand. Third, more than 90% of our responses correspond to brands known by our participants—thereby justifying our selection of the brands covered in our main paper.

7 Extended Logo Experiments

Brands with "Few-shot" Logos. Intuitively, the attack difficulty may be related to the number of different logos each brand has. For example, brands with more logos may allow PhishIntention to learn a more robust embedding for the brand (i.e., harder to attack). We plot the result for the 110 brands in Figure 12: each point represents a given brand, the y-axis
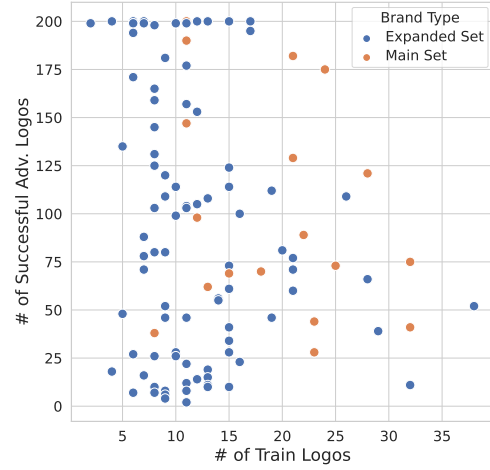

Figure 12: **# of Successful Adv. Logos vs. # Training Logos in PhishingIntention** —We show a scatter plot to examine the relationship between the number of training logos each brand has for PhishingIntention (X) and the number of successful adversarial logos identified by `LogoMorph` (Y).

reports the number of successful logos, and the x-axis the number of logos included in PhishIntention's training set for that brand. First, we see that brands with fewer logos (e.g., less than 10) are not necessarily easier or harder to attack since the number of successful attack logos varies between 0–200. Second, brands with more logos (e.g., more than 25) seem to be harder to attack. We run a Pearson correlation analysis on these two variables and resulting $r = -0.12, p = 0.21$. While it exhibits a negative correlation, the high p value (> 0.05) means the observed correlation is not statistically significant.

> **Takeaway.** There is no significant evidence supporting the fact that the number of logos included in the training set for a brand is a significant factor in predicting the effectiveness of using `LogoMorph` against such a brand.

References

[1] APRUZZESE, G., CONTI, M., AND YUAN, Y. Spacephish: The evasion-space of adversarial attacks against phishing website detectors using machine learning. In *Proc. of ACSAC* (2022).

[2] BAKI, S., AND VERMA, R. M. Sixteen years of phishing user studies: What have we learned? *IEEE Transactions on Dependable and Secure Computing 20*, 2 (2022), 1200–1212.

[3] CARLINI, N., AND WAGNER, D. A. Towards evaluating the robustness of neural networks. In *Proc. of IEEE SP* (2017).

[4] CHIEW, K. L., CHANG, E. H., TAN, C. L., ABDULLAH, J., AND YONG, K. S. C. Building standard offline anti-phishing dataset for benchmarking. *International Journal of Engineering & Technology* (2018).

[5] DRAGANOVIC, A., DAMBRA, S., IUIT, J. A., ROUNDY, K., AND APRUZZESE, G. "do users fall for real adversarial phishing?" investigating the human response to evasive webpages. In *APWG 2023 eCrime Symposium* (2023).

[6] HO, J., JAIN, A., AND ABBEEL, P. Denoising diffusion probabilistic models. In *Proc. of NeurIPS* (2020).

[7] LEE, J., XIN, Z., SEE, M., SABHARWAL, K., APRUZZESE, G., AND DIVAKARAN, D. M. Attacking logo-based phishing website detectors with adversarial perturbations. In *Proc. of ESORICS* (2023).

[8] LIN, Y., LIU, R., DIVAKARAN, D. M., NG, J. Y., CHAN, Q. Z., LU, Y., SI, Y., ZHANG, F., AND DONG, J. S. Phishpedia: A hybrid deep learning based approach to visually identify phishing webpages. In *Proc. of USENIX Security* (2021).

[9] LIU, R., LIN, Y., YANG, X., NG, S. H., DIVAKARAN, D. M., AND DONG, J. S. Inferring phishing intention via webpage appearance and dynamics: A deep vision based approach. In *Proc. of USENIX Security* (2022).

[10] LUO, C. Understanding diffusion models: A unified perspective. In *arXiv preprint arXiv:2208.11970* (2022).

[11] NICHOL, A. Q., AND DHARIWAL, P. Improved denoising diffusion probabilistic models. In *Proc. of ICML* (2021).